Fluorescent eco-particles for surface flow physics analysis

F. Tauro, M. Porfiri, and S. Grimaldi

Citation: AIP Advances **3**, 032108 (2013);
View online: https://doi.org/10.1063/1.4794797
View Table of Contents: http://aip.scitation.org/toc/adv/3/3
Published by the American Institute of Physics

Fluorescent eco-particles for surface flow physics analysis

F. Tauro,[1,2,3] M. Porfiri,[1,a] and S. Grimaldi[1,3,4]
[1]*Department of Mechanical and Aerospace Engineering, Polytechnic Institute of New York University, Brooklyn, NY 11201, USA*
[2]*Dipartimento di Ingegneria Civile, Edile e Ambientale, Sapienza University of Rome, Rome 00184, Italy*
[3]*Honors Center of Italian Universities, Sapienza University of Rome, Rome 00184, Italy*
[4]*Dipartimento per l'Innovazione nei Sistemi Biologici, Agroalimentari e Forestali, University of Tuscia, Viterbo 01100, Italy*

(Received 1 November 2012; accepted 12 February 2013; published online 1 March 2013)

In this letter, we describe a novel methodology for fabricating inexpensive environmentally-friendly fluorescent microparticles for quantitative surface flow visualization. Particles are synthesized from natural white beeswax and a highly diluted solution of a nontoxic fluorescent red dye. Bead fluorescence exhibits a long lifetime in adverse conditions, such as exposure to weathering agents, and is enhanced by Ultra Violet radiation. The fluorescent eco-particles are integrated in a particle image velocimetry study of circular hydraulic jump to demonstrate their feasibility in tracing complex surface flows. *Copyright 2013 Author(s). This article is distributed under a Creative Commons Attribution 3.0 Unported License.* [http://dx.doi.org/10.1063/1.4794797]

Quantitative flow visualization techniques, such as particle image velocimetry (PIV), are based on seeding the fluid with small tracers and analyzing consecutive images of their motion.[1] These methodologies are highly dependent on the ability of the particles to reliably trace the flow and on the image quality, which, in turn, is severely affected by particles' visibility. The latter is of fundamental importance for particle tracing systems in outdoor measurements, where unpredictable flow and light settings, variable topography of the fluid free surface, light reflections, and restrictions in tracer deployment are relevant.[8] Beyond being visible in outdoor conditions, surface tracers for environmental studies should be nontoxic, buoyant, and chemically stable and should have low detection limit and negligible sorption affinity to natural substrates.[13]

In this framework, considerable efforts have been devoted to the fabrication of fluorescent particle tracers with dimensions ranging from few tens of nanometers to few millimeters for integration in traditional PIV;[16] total internal reflection velocimetry;[9] three-dimensional interfacial PIV;[21] and particle streak velocimetry.[10,17] These studies demonstrate the potential of using fluorescence for reducing the effect of adverse illumination and support the feasibility of synthesizing inexpensive particle tracers for laboratory controlled flow experiments. Nevertheless, environmentally-friendly and neutrally buoyant fluorescent tracers for surface flow physics analysis are yet to be developed.

In this letter, we describe a novel methodology for fabricating inexpensive environmentally-friendly fluorescent particles for quantitative flow visualization. Particles are synthesized from natural beeswax and a highly diluted solution of a nontoxic fluorescent red dye. The fabrication procedure allows for adjusting the size of the particles from tens of microns up to a few millimeters and their density from positively to negatively-buoyant with respect to water. An array of experimental techniques is employed to conduct a thorough characterization of the fluorescence and morphology of the tracers. In addition, ad-hoc experiments are designed to assess the fluorescence response due

[a]mporfiri@poly.edu; http://faculty.poly.edu/~mporfiri/index.htm

to Ultra Violet (UV) exposure and thermal processes. A proof-of-concept PIV study is conducted to illustrate the integration of the novel particle tracers in existing velocimetry methods for surface flow analysis.

Particles are synthesized from natural white beeswax pellets purchased from Stakich Inc., MI., whose density is approximately equal to 0.95 g/cm^3. A batch of 20 g of beads is obtained by melting 23 g of wax at $60^\circ - 65^\circ$ C through a thermostatic bath and by stirring them at 350 rpm until melting is achieved. A 6×10^{-3} μg/l diluted solution is prepared from nontoxic Fluorescent FWT Red Dye Concentrate, Cole Parmer®. A volume of 8 ml of diluted solution and 1 ml of surfactant Polysorbate-20, 1.1 g/cm^3 in density, are added to the melted wax and stirred at 350 rpm until homogeneous mixing is achieved. The emulsion is then poured in 100 ml of hot water at $60^\circ - 65^\circ$ C and kept under stirring at 600 rpm for $3 - 4$ minutes to facilitate the formation of wax drops. After drop formation, 125 ml of cold water at 5° C are added to the mixture and stirring is stopped. Cold water produces the instantaneous cooling of the wax drops that solidify and migrate to the surface of the suspension. Particles are then collected through filtering with a 20 μm sieve and desiccated with silica gel for 48 hrs. The diameters of the beads obtained with a stirring frequency of 600 rpm range from less than 20 to 500 μm. In particular, 40% of the particles lie in the range $250 - 420$ μm. The size of the beads can be adjusted by regulating the frequency of the rotation of the magnetic stirrer in the emulsion of wax and hot water. Specifically, higher frequencies lead to smaller particles, whereas frequencies as low as 300 rpm produce particles of a few millimeters. Particles are positively buoyant in water, yet, negatively-buoyant beads can be obtained by following a similar fabrication procedure where quantities of calcium carbonate of density in the range $2.7 - 2.8$ g/cm^3 are added to the emulsion of beeswax and fluorescent solution. Due to the low affinity of beeswax for calcium carbonate, diluted solutions of surfactant should be added to the emulsion and stirring performed for several minutes. The amount of calcium carbonate added to the emulsion can be adjusted to vary the density of the particles. In particular, particles are found to sink in water when amounts of calcium carbonate greater than 5 mg are released in the 100 ml hot emulsion. Advanced fabrication methods for mechanical emulsification based on high pressure or ultrasound homogenizers, microporous membranes, and microfluidizers[22] are expected to be relevant towards the massive production of fluorescent particle tracers of highly controlled shape and size. However, the need for regulating the temperature of the beeswax emulsion to guarantee the complete mixing of the matrix with the dye is anticipated to pose severe challenges in adapting such advanced methods.

When compared with the state of the art on tracers for surface flow physics analysis, the proposed fluorescent beeswax particles demonstrate several advantages. Differently from polyethylene, titanium, aluminum, and silver particles typically used in PIV,[14,18] beeswax is biodegradable with natural biodegradation time of 28 days.[7] Moreover, fluorescent FWT Red Dye Concentrate is nontoxic in contrast with fluorescent tracers traditionally used in environmental studies, such as Rhodamine WT, Rhodamine B, and Fluorescein.[13] Finally, the proposed particles can be inexpensively fabricated at a limited cost of 0.025 \$/g in contrast with commercially available fluorescent particles, whose costs[3] range from 0.8 \$/g to 9.9 \$/g.

The morphology of the synthesized particles is studied by using scanning electron microscopy (SEM). Fluorescent particles with diameters ranging from 250 to 420 μm are coated with a 50 nm layer of gold and analyzed through the Hitachi S-3400N VP-SEM. Images are acquired by setting the accelerating voltage to 5 kV and the working distance to 10.9 mm. Figure 1 displays three SEM images at 270 x, 1.7 kx, and 95 kx magnification, respectively. Particles' shape is found to be approximately spherical with surface microfeatures attributable to the instantaneous cooling of the wax emulsion during fabrication. Moreover, Figure 1 offers evidence that the fabrication method produces particles of comparable size and shape as indicated above. The particle microstructure is studied by analyzing the diffraction spectra of both the beads and the unprocessed beeswax. X-ray spectra of beeswax pellets and fluorescent particles, measured using Rigaku Miniflex X-Ray Diffractometer and recording at diffraction angles from 10° to 70°, are found to be similar (peaks in unprocessed wax and fluorescent particles' spectra occur at the same diffraction angles: $2\phi = 19^\circ$, 21°, 24°, 30°, 36°, 40°, 47°, and 52° and the variation between the two spectra is at most 20% at each peak) thus confirming the minimal presence of dye in the bead matrix. In addition, characteristic

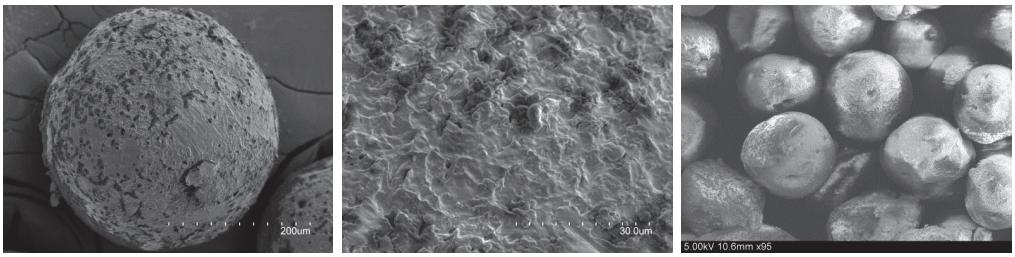

FIG. 1. SEM picture of the fluorescent particles. (a) low magnification image of an individual particle; (b) higher magnification view displaying surface morphology details; and (c) low magnification image of a group of beads.

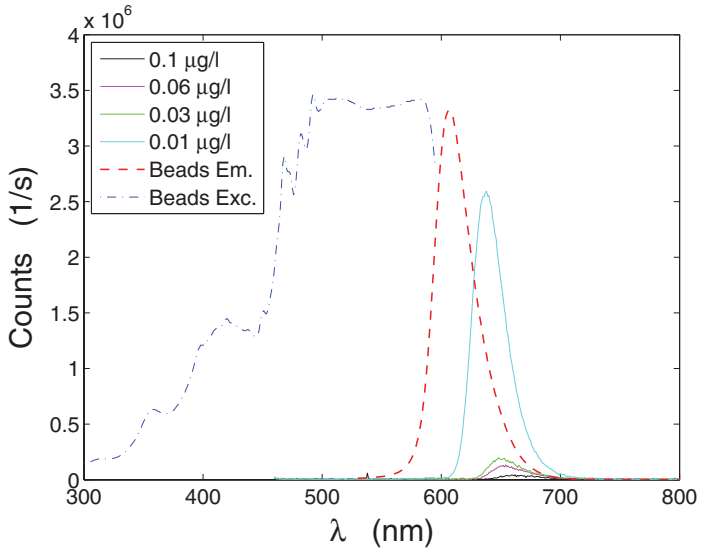

FIG. 2. Fluorescence spectra measured with PTI Quanta Master 40 spectrofluorometer. Solid lines are emission spectra for diluted solutions of the fluorescent dye; spectra are multiplied by 100 for legibility. Dashed-dotted blue line refers to the beads excitation spectrum and dashed red line to the beads emission spectrum.

peaks in the diffraction spectra suggest that polycrystalline structure and crystal size of beeswax[4] are preserved during the fabrication procedure.

The characterization of the particle fluorescence is performed by conducting excitation and emission scans of solutions at different concentrations of Fluorescent FWT Red Dye and particle samples with PTI Quanta Master 40 spectrofluorometer. Specifically, diluted liquid solutions are prepared by varying the dye concentration from 0.01 to 0.1 μg/l. The emission scan of liquid solutions with excitation at 450 nm results in the spectra displayed in Figure 2, where emissions are multiplied by 100 for improved readability. It is noted that more diluted solutions lead to higher fluorescence quantum yields accompanied by shifts towards lower wavelengths. Such behavior is attributed to collisional quenching effects which are typical of the rhodamine-family dyes.[6,11,12] Figure 2 also reports the emission and excitation scans for a volume of 2 ml of melted fluorescent particles. Notably, particles present a broad excitation spectrum which allows for stronger fluorescence under a wide range of wavelengths. This is crucial for conducting experiments in natural flow systems where sunlight can be used as the excitation source.[18–20] In addition, particle emission spectrum is shifted towards lower wavelengths with a higher peak as compared to diluted solutions of the fluorescent dye. This is likely due to collisional effects' reduction from mixing wax and water with

the highly diluted dye solution during the fabrication procedure, which contributes to decreasing the concentration of fluorophore molecules in the particles.

The effects of weathering agents on the lifetime and intensity of the particle fluorescence emissions are assessed by exposing beads to high-energy radiations and hot water and periodically measuring their emission through GloMax®-Multi Jr fluorometer. These nondestructive experiments are performed on the solid unmelted beads and, thus, preserve the total surface subject to external agents. The effect of high-energy light on the particle fluorescence is studied by continuously exposing ten samples of 0.5 g of beads to an 8 W UV lamp, 365 nm in wavelength, for two weeks. During the experiment, beads are stored in ten labeled petri dishes in an opaque environment at 15 cm below the UV lamp. Each sample is transferred in plastic methacrylate 10×10 mm cuvette containers to perform the measurement. Before testing, samples are tapped to guarantee that the particles are closely packed in the cuvettes and, therefore, limit the presence of voids that may bias the optical data. The intensity of the fluorescence emission is measured with two optical kits: the green module (excitation wavelength: 525 nm and emission wavelength: $580 - 640$ nm) and the UV-GFP module (excitation wavelength: 365 nm and emission wavelength: $515 - 570$ nm). Every other day, five acquisitions are taken at intervals of two seconds with both optical modules on each sample and averaged to characterize the sample behavior. Unexpectedly, the data recorded at the end of the two weeks are on average three times the initial values recorded with the green module and two times the values obtained with the UV-GFP kit.

Such time dependence is studied by performing a repeated measures analysis of variance on the collected data (ten particle samples and seven repeated measures for each sample). The analysis reveals a statistically significant time-effect (level of significance <0.0001) suggesting that exposure to UV light modulates particle fluorescence. An additional test performed with PTI Quanta Master 40 spectrofluorometer at the end of the UV ray exposure allows for further investigating the increase in the emissions. Specifically, four samples of particles previously exposed to UV light are melted and used for emission scanning. The peak of the emission spectrum is shifted to 592 nm and the intensity is comparable to the maximum intensity detectable by the instrument (3.76×10^6 1/s). Such phenomena are likely attributed to photobleaching effects induced by the high-energy rays which tend to degrade fluorophore molecules.[5,15] A decrease in fluorescing molecules leads to reduced collisional quenching and, therefore, higher fluorescence quantum yield. These conclusions are confirmed by visual inspection of UV-exposed beads which present a faded pink coloring, suggesting that fluorophore molecules in the external layer of the particles are degraded by the high-energy light radiation.

The effect of hot water on particle fluorescence is evaluated by deploying a sample of 0.5 g of beads in 100 ml of tap water at 50° C. Particles are continuously kept in hot water and under magnetic stirring at 350 rpm for 12 hours a day for two weeks. Fluorescence measurements are performed by filtering the suspension, desiccating the beads with silica gel for a few hours, and then transferring the sample in a methacrylate cuvette for acquisitions with GloMax®-Multi Jr fluorometer. Every other day, the emission intensities of the samples are analyzed following the procedure presented above. In particular, values measured with the green module are reduced of 91% and data recorded with the UV-GFP kit show a decrease of 84%. An additional test performed on the melted material with PTI Quanta Master 40 spectrofluorometer does not display significant peaks in the emission spectrum. More specifically, the material is not fluorescent when excited under a broad range of wavelengths. This suggests that fluorophore molecules are degraded and washed out during the thermal treatment as qualitatively confirmed by the opaque cyan coloring of the beads at the end of the experiment.

The ability of the particles to trace complex surface flows is investigated by performing a proof-of-concept PIV laboratory experiment on the circular hydraulic jump generated by a water jet impacting a rigid wall. Hydraulic jump is studied using the setup in Figure 3, where water is recirculated through a piping system via a submersible Beckett Corp G210AG20 210 GPH pump and regulated through a diverting three-port ball valve and a butterfly valve. An electronic GPI A109GMN025NA1 digital flow meter is placed at proper distances from the valves to monitor the flow discharge. The jet is spread out from a brass straight-hose tapered nozzle, whose output diameter, $2a$, is equal to 5 mm. The nozzle is located 5 cm above a horizontal 30×30 cm polycarbonate plate. The plate rests on the bottom of a water tank through four aluminum legs; the lower side of the plate

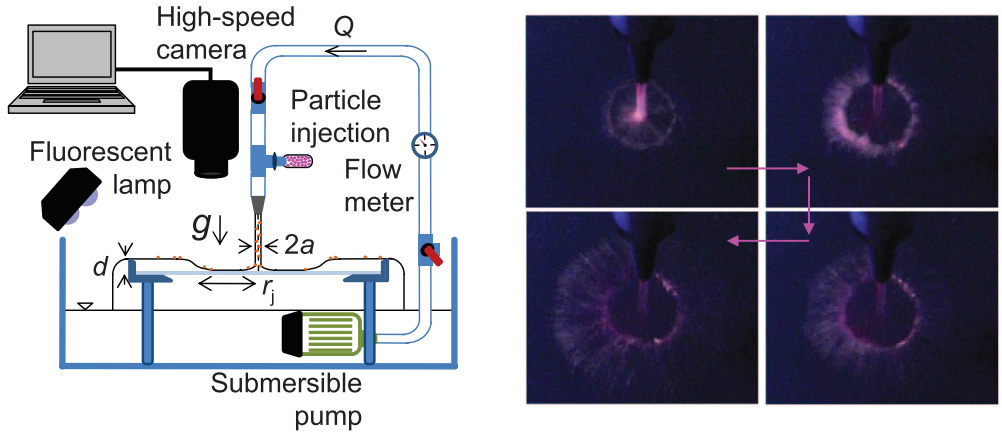

FIG. 3. Left, experimental setup for the circular hydraulic jump experiment and right, snapshots depicting particle tracer ejection on the horizontal plate.

is covered with opaque material to enhance the fluorescence of the beads and improve their visibility. The depth of the water on the horizontal surface, d, is set to 2.5 mm through aluminum L-brackets installed along the edges of the plate. During each experiment, a few grams of fluorescent particles are seeded into the flow through an injection system and ejected through the nozzle onto the plate. A fluorescent 50 W lamp placed along a side of the water tank at 5 cm from the water surface excites the particle fluorescence. Figure 3 shows the particle motion for a representative case scored with a CMOS Canon VIXIA HG20 camcorder at approximately 50 cm from the plate.

PIV analysis are conducted with an IDT MotionPro 3 Series 1 k $\times$ 1 k pixel color CMOS camera placed at 14 cm from the plate for image acquisition. Camera acquisition frequency is set to 300 Hz, exposure time to 2353 μs, and sensor gain to +6 dB. PIV experiments are performed by varying the flow rate from 2.5 $\times$ 10^{-5} to 6.7 $\times$ 10^{-5} m^3/s in increments of 0.8 $\times$ 10^{-5} m^3/s. After acquisition, a sequence of 50 frames sampled at intervals of 6.67 ms from the entire sequence of 2000 frames of a single experiment is used for processing. The sequence of 50 frames illustrates the trajectory of the particles from the impact of the water jet to few centimeters outside the circle. The processed field of view is equal to 7 $\times$ 8 cm where the physical dimension of 1 cm corresponds to 122 pixels in images. The sequence of frames is analyzed through ed-PIV software. Each image is subdivided into 32 $\times$ 32 pixels interrogation regions and cross-correlation is performed using a multi-pass fast Fourier transform.

For the analysis, a polar coordinate system is defined such that the origin is located at the center of the impact of the jet and the angle θ spans from 0° to 180°, see Figure 4. After PIV processing, the radial component of the flow velocity is obtained and averaged over the 50 pairs of frames. Figure 4 depicts the contours of the time-averaged radial velocity field for the flow discharge 5.83 $\times$ 10^{-5} m^3/s. It is observed that the velocity inside the circular jump is much larger than outside; thus, particles in this inner region are scored as oblate ellipses, limiting the accuracy of PIV therein. This results in null velocity values inside the circular jump, see the blue contours inside the jump showed in Figure 4. Higher camera acquisition frequencies would be necessary to obtain better quality pictures and apply PIV inside the circle. On the other hand, particles are clearly visible outside the jump and they allow for reliably estimating the velocity field. The radial velocity field is experimentally estimated by computing time-averaged radial velocity profiles as a function of the distance from the jet impact for sectors of 10° spanning from $\theta = 45°$ to $\theta = 135°$, see Figure 4. Such sectors are selected due to the fact that they are located underneath the camera lens and are not affected by optical distortion and scarce illumination issues. The maximum radial velocity value in the 90° sector is referred to as U and the radius at which it is attained is termed r_{max}. As a validation of PIV measurement, Fig. 5 compares the direct measurement of the flow discharge $Q^\star$ with its estimate $Q = U(2\pi r_{max} d)$ obtained PIV data. Results reported therein indicate that ratio between PIV and direct measurement is 0.860 with a standard deviation of 0.239, thus supporting

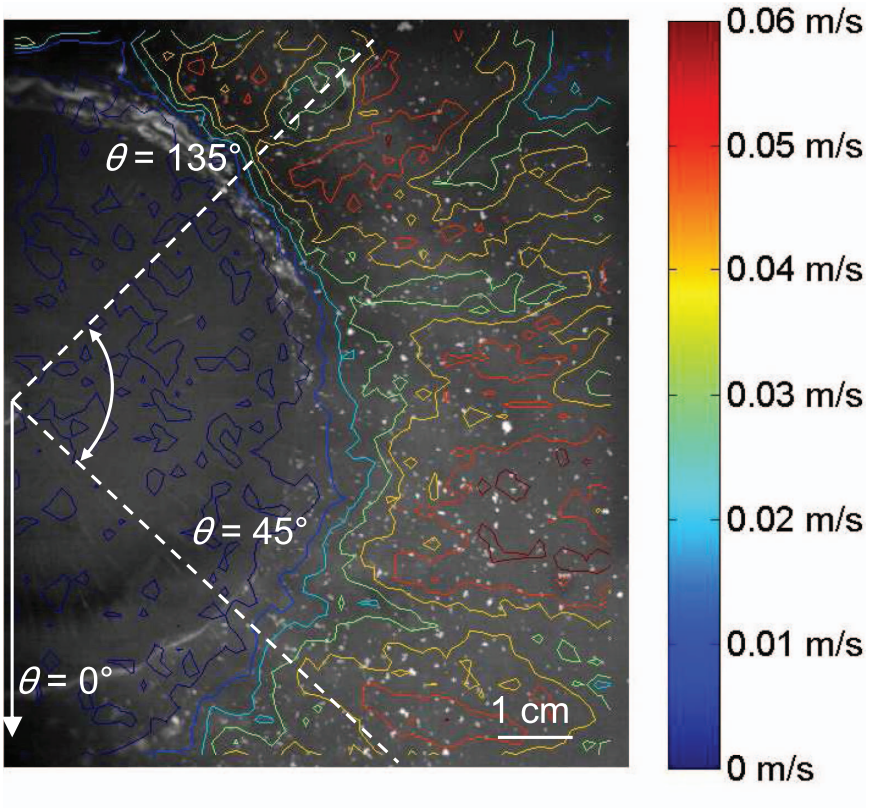

FIG. 4. Radial flow velocity field for the circular hydraulic jump experiment depicting the polar coordinate system used for analysis. Flow discharge is 5.8×10^{-5} m^3/s.

the feasibility of using the proposed particles to study hydraulic jump especially for smaller values of flow discharges.

To further investigate the potential of the proposed tracers in studying surface flow physics, PIV images are further analyzed to extract the radius of the circular jump[23] r_j, which is then used in conjunction with the estimate of the flow discharge Q to partially validate the model presented in Ref. 23. Specifically, it therein demonstrated that r_j depends on relevant flow parameters through

$$\frac{r_j d^2 g a^2}{Q^2} + \frac{a^2}{2\pi^2 r_j d} = 0.01676 \left[\left(\frac{r_j}{a} \right)^3 R^{-1} + 0.1826 \right]^{-1} \tag{1}$$

for $(r_j/a)R^{-1/3} \geq 0.3155$, and

$$\frac{r_j d^2 g a^2}{Q^2} + \frac{a^2}{2\pi^2 r_j d} = 0.10132 - 0.1297 \left(\frac{r_j}{a} \right)^{\frac{3}{2}} R^{-\frac{1}{2}} \tag{2}$$

for $(r_j/a)R^{-1/3} < 0.3155$, where g is the gravitational acceleration and R is the jet Reynolds number, which is defined as $R = Q/\nu a$ with ν being the kinematic viscosity of water. Comparison with theoretical results is presented in Figure 5 where relations (1) and (2) are presented as a solid curve and markers refer to experimental results. Following Ref. 2, the left hand sides of Eqs. (1) and (2) are plotted against $(r_j/a)^3 R^{-1}$ to facilitate comparison. The theoretical prediction in Ref. 23 is found to generally overestimate experimental results with an error which increases as the Reynolds number increases. Similar evidence is reported in Ref. 23, where measurements are obtained without using a PIV system, yet, discrepancies between experimental and theoretical results observed therein are smaller than those found in this study. Such discrepancies may be due to theoretical factors, such as neglecting fluid surface tension,[2] and experimental uncertainties associated to PIV practice, including spatial heterogeneities in particle seeding, light reflections from the water surface, distortions from

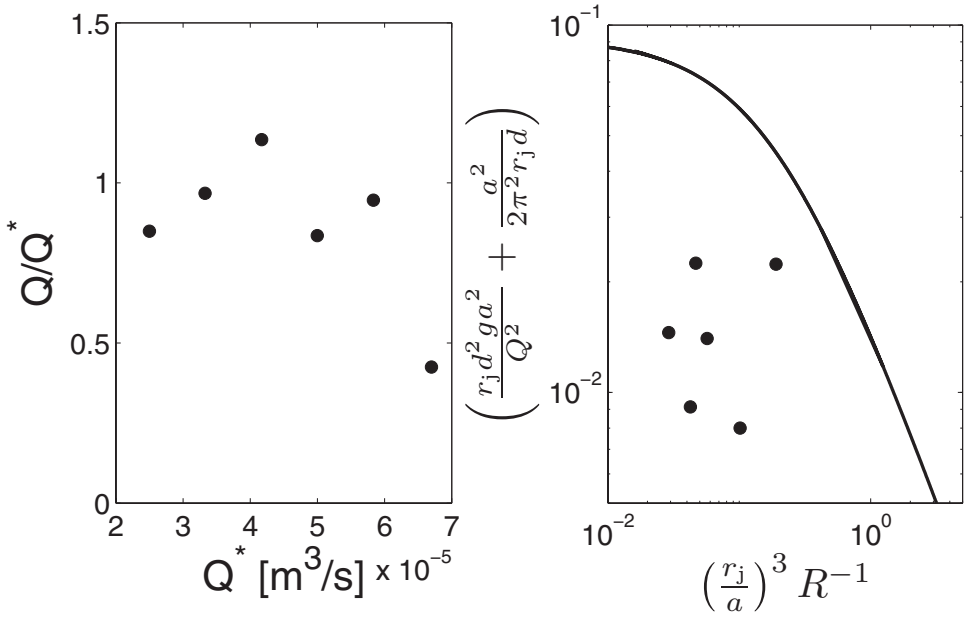

FIG. 5. Left, validation of the velocity measurement obtained using PIV. Right, comparison between theoretical prediction as proposed in Ref. 23, solid line, and experimental observations, markers, obtained from PIV measurements.

the camera lenses, and unfavorable illumination conditions as compared to the high acquisition frequency.

In conclusion, we presented a novel procedure for fabricating low-cost, high-visibility, and environmentally-friendly particle tracers for surface flow investigations. Particle fluorescence was found to exhibit a long lifetime and to be enhanced by high-energy illumination which is typical of natural settings. A proof-of-concept PIV experiment conducted on the circular hydraulic jump generated by a water jet impacting a rigid wall demonstrated the feasibility of the tracer in measuring surface velocity in complex flows.

ACKNOWLEDGMENTS

This research was partially supported by the Honors Center of Italian Universities, the MIUR project PRIN 2009 N. 2009CA4A4A, and the National Science Foundation under grant numbers CMMI-0745753 and CMMI-0926791. The authors also acknowledge the support of the Office of Naval Research through grant number N00014-10-1-0988 that has allowed the acquisition of equipment used in this study. The authors are also grateful to Mr. Emiliano Rapiti for help with particle fabrication, Dr. Jin R. Kim for providing the opportunity of using PTI Quanta Master 40 spectrofluorometer, and Drs. Nikhil Gupta, Simone Macrì, and Sean D. Peterson for thoughtful discussions.

[1] R. J. Adrian, "Twenty years of particle image velocimetry," Exp. Fluids **39**(2), 159–169 (2005).
[2] J. W. M. Bush and J. M. Aristoff, "The influence of surface tension on the circular hydraulic jump," J. Fluid Mech. **489**, 229–238 (2003).
[3] Cospheric LLC, http://www.cospheric-microspheres.com/default.asp, 2010.
[4] D. L. Dorset, "Development of lamellar structures in natural waxes - an electron diffraction investigation," J. Phys. D **32**, 1276–1280 (1999).
[5] C. Eggeling, A. Volkmer, and C. A. M. Seidel, "Molecular photobleaching kinetics of rhodamine 6G by one- and two-photon induced confocal fluorescence microscopy," ChemPhysChem **6**, 791–804 (2005).
[6] M. Fikry, M. M. Omar, and L. Z. Ismail, "Effect of host medium on the fluorescence emission intensity of rhodamine B in liquid and solid phase," J. Fluoresc. **19**(4), 741–746 (2009).
[7] A. O. Hanstveit, "Biodegradability of petroleum waxes and beeswax in an adapted CO_2 evolution test," Chemosphere **25**(4), 605–620 (1992).

[8] A. Hauet, A. Kruger, W. Krajewski, A. Bradley, M. Muste, J. D. Creutin, and M. Wilson, "Experimental system for real-time discharge estimation using an image-based method," J. Hydrol. Eng. **13**(2), 105–110 (2008).
[9] S. Jin, P. Huang, J. Park, J. Y. Yoo, and K. S. Breuer, "Near-surface velocimetry using evanescent wave illumination," Exp. Fluids **37**(6), 825–833 (2004).
[10] L. Kemp, E. C. Jamieron, and S. J. Gaskin, "Phosphorescent tracer particles for lagrangian flow measurement and particle tracking velocimetry," Exp. Fluids **48**(5), 927–931 (2010).
[11] M. Kubista, R. Sjöback, S. Eriksson, and B. Albinsson, "Experimental correction for the inner-filter effect in fluorescence spectra," Analyst **119**(3), 417–419 (1994).
[12] A. Kurian, N. A. George, B. Paul, V. P. N. Nampoori, and C. P. G. Vallabhan, "Studies on fluorescence efficiency and photodegradation of rhodamine 6G doped PMMA using a dual beam thermal lens technique," Laser Chem. **20**(2–4), 99–110 (2002).
[13] C. Leibundgut, P. Maloszewski, and C. Külls, *Tracers in Hydrology* (Wiley-Blackwell, Oxford, UK, 2009).
[14] A. Melling, "Tracer particles and seeding for particle image velocimetry," Measurement Science and Technology **8**(12), 1406–1416 (1997).
[15] M. Nakanishi, O. Sugihara, N. Okamoto, and K. Hirota, "Ultraviolet photobleaching process of azo dye doped polymer and silica films for fabrication of nonlinear optical waveguides," Appl. Optics **37**(6), 1068–1073 (1998).
[16] F. Pedocchi, J. Martin, and M. H. García, "Inexpensive fluorescent particles for large-scale experiments using particle image velocimetry," Exp. Fluids **45**(1), 183–186 (2008).
[17] M. S. Pervez and T. H. Solomon, "Long-term tracking of neutrally buoyant tracer particles in two-dimensional fluid flows," Exp. Fluids **17**(3), 135–140 (1994).
[18] F. Tauro, S. Grimaldi, A. Petroselli, and M. Porfiri, "Fluorescent particle tracers in surface hydrology: a proof of concept in a natural stream," Water Resour. Res. **48**, W06528, doi:10.1029/2011WR011610 (2011).
[19] F. Tauro, S. Grimaldi, A. Petroselli, M. C. Rulli, and M. Porfiri, "Fluorescent particle tracers in surface hydrology: a proof of concept in a semi-natural hillslope," Hydrol. Earth Syst. Sci. **16**, 2973–2983 (2012).
[20] F. Tauro, C. Pagano, M. Porfiri, and S. Grimaldi, "Tracing of shallow water flows through buoyant fluorescent particles," Flow Meas. Instrum. **26**, 93–101 (2011).
[21] D. E. Turney, A. Anderer, and S. Banerjee, "A method for three-dimensional interfacial particle image velocimetry (3D-IPIV) of an air-water interface," Meas. Sci. Technol. **20**(4), 045403 (2009).
[22] G. T. Vladisavljević, U. Lambrich, M. Nakajima, and H. Schubert, "Production of O/W emulsions using SPG membranes, ceramic α-aluminum oxide membranes, microfluidizer and a silicon microchannel plate - a comparative study," Colloid. Surface. A **232**(2–3), 199–207 (2004).
[23] E. J. Watson, "The radial spread of a liquid jet over a horizontal plane," J. Fluid Mech. **20**, 481–499 (1964).